

The complex structure and peculiar internal motions of the planetary nebula NGC 6210

1

November 5, 2019

ABSTRACT

A comprehensive kinematic study has been carried out on the planetary nebula (PN) NGC 6210. Multiple long-slits, echelle spectra have been obtained over the face of this nebula mapping its full shell structure, the opposite pairs of extended, twisted arms and the bipolar collimated outflows and bullets. Public *HST* imagery has been used to identify kinematic elements with structural components. The long-slit spectroscopic information has been combined into channel maps that greatly facilitate visualizing the otherwise intricate expansion pattern of this planetary nebula. The global morphology of NGC 6210 is reminiscent of other planetary nebulae with extended X-ray emission, suggesting the presence of a central hot bubble produced by shocked stellar wind. In spite of the dramatic structure of this PN substantial expanding radial motions are only found in the material surrounding the central, inner shell. The slow radial motions of the collimated outflows and the bullet-like knots indicate that they are moving away from the core very close to the plane of the sky, nearly perpendicular to the line of sight

Key words. Planetary Nebulae: individual (NGC 6210) – ISM: kinematics and dynamics – ISM jets and outflows – techniques: spectroscopy

1. INTRODUCTION

NGC 6210 is a bright and relatively large PN in the northern sky. The first photographic image of NGC 6210 was published by Duncan (1937). In this old, fuzzy, image the twisted arms protruding from the bright core of the nebula are apparent. Several studies have discussed possible kinematic models for this object (Osterbrock et al. 1966; Weedman 1968; Becker, Giesecking and Solf, 1984; Icke, Preston and Balick, 1987). None of these studies had both, the spatial coverage and spectral resolution needed to produce a reliable spatio-kinematic model of this PN. More recently, Cuesta & Phillips (1992) obtained 8 long-slits throughout the face of the nebula with but with only limited, medium spectral resolution. From these data and the already available *HST* images at the time they suggested a reasonable kinematic model for NGC 6210. NGC 6210 jumped into fame from the *HST* images obtained K. Borkowski (1996) program No XXX and Robert Rubin (1997-1998) program YYYY. These images showed for the first time the extraordinary complex looking morphology of NGC 6210. Hajian, Terzian and Bignell (1995) derive a distance to NGC 6210 from expansion parallax of xxx whereas . We shall the later distance (GAIA?)

In this work we present the most complete and thorough mapping of all the morphological structures of the PN, obtained at high spectral resolution. These data allow us to disentangle the various spatio-kinematic components and provide an overall view of its evolution.

The planetary nebula NGC 6210 is also known as "the turtle" given its main body and extended arms that resemble the shell of a turtle and its fins. Its very complex structure was revealed by an image obtained by

servatorio Astronómico Nacional at San Pedro Mártir, (OAN-SPM), Baja California, México. We used the Manchester Echelle Spectrometer (MES-SPM) (Meaburn et al. 2003) on the 2.1 m telescope in its $f/7.5$ configuration. The MES-SPM is a long-slit, echelle spectrometer that has no cross-disperser; it isolates single orders using interference filters. For the 2003, 2004 and 2011 of the present observations, we used a SITE-3 CCD detector with 1024×1024 square pixels, each $24 \mu\text{m}$ on a side ($\equiv 0.312 \text{ arcsec pixel}^{-1}$). The detector was set to a binning of 2×2 in both the spatial and spectral directions. Consequently, 512 increments, each $0''.624$ long gave a projected slit length of 5.32 on the sky. A TEK-1 CCD detector was used for the 1998 data set with 1024×1024 pixels² with sides measuring $24 \mu\text{m}$, using 2×2 binning ($\equiv 0.62 \text{ arcsec pixel}^{-1}$ and $3.5 \text{ km s}^{-1} \text{ pixel}^{-1}$). For the 2001 and 2013 we used a Marconi CCD detector with 2048×2048 square pixels, each $13.6 \mu\text{m}$ on a side. The detector was set to a binning of 2×2 in both the spatial and spectra directions. Consequently, 1024 increments, each $0''.352$ long gave a projected slit length of 5.47 on the sky.

We used a 90 \AA and 50 \AA bandwidth filter to isolate the 87th and 114th orders containing the $\text{H}\alpha + [\text{N}2] 6584$ and $[\text{O}3] 5007 \text{ \AA}$ nebular emission lines, respectively. We used a $70 \mu\text{m}$ ($\equiv 0.95''$) slit, giving a velocity resolution of 9.2 km s^{-1} ($\equiv 0.312 \text{ arcsec pixel}^{-1}$ and $150 \mu\text{m}$ ($\equiv 1''.9$ and $\equiv 11.5 \text{ km s}^{-1}$) slit).

We obtained 23 consecutive and tightly spaced positions over the NGC 6210. The slit positions are indicated and labeled in Figure 1 on a WFPC 2 image of the NGC 6210 obtained from the HST archive. In order to establish the exact position of the slit in each pointing, the slit position on the sky was recorded with an automatic procedure available in MES-SPM prior to the spectroscopic exposure.

The log of spectroscopy observation is given in Table 1 divided into dates, number of spectra, exposure times, spectral range, resolution, slit wide, position angle and name of the slit

2. OBSERVATIONS AND DATA REDUCTION

Long-slit, echelle, spectroscopic observations of the nebula NGC 6210 were performed with the 2.1 m telescope at the Ob-

(see Figure 1). The high resolution data are available in San Pedro M  rtir Kinematic Catalogue of Galactic Planetary Nebulae (<http://kincatpn.astrosen.unam.mx>) (L  pez et al. 2012).

Due to saturation of several slit positions on the nebula, we obtained a new set of observation on August 13, 2015. We used the same detector as that used for the 2015 dataset, which was a E2V-4240 (Marconi 2) detector with 2048×2048 pixels² with sides measuring $13.5 \mu\text{m}$, using 2×2 binning ($\equiv 0.531 \text{ arcsec pixel}^{-1}$). Spectra were obtained at 11 different positions across the nebula, with exposure times of 1800 seconds. The slit was oriented N-S. The characteristics of the observations are listed in Table 2.

All data was reduced (bias removal and cosmic-ray removal) by using standard IRAF¹. This was followed by rectification and first-order wavelength calibration of the two-dimensional spectra based on the comparison the spectrum of a Th/Ar lamp to an accuracy of $\pm 1 \text{ km s}^{-1}$ when converted to radial velocity. All spectra presented in this paper are corrected to heliocentric velocity (V_{hel}). The Figures ??, ??, and show the position-velocity ($P-V$) arrays of H α 6563 Å [N 2] 6584, [O 3] 5007 Å, respectively, where the heliocentric velocities are used, and positions are specified as arcsecond offsets (x,y).

Using FORTRAN and python routines, we produced velocity cubes in [N 2] 6584 and H α emission lines, in order to

The resulting data cubes for the H α 6563 Å and [N 2] 6584 lines are shown in Figure 3 as isovelocity channel maps, each isovelocity map is 20 km s^{-1} wide.

3. KINEMATICS

The Figure 2 shows the H α 6563 Å, [N 2] 6584 and [O 3] 5007 Å $P-V$ arrays for all individual slit position, observed on 2015 epoch: H α $P-V$ is shown on the left panel, on the middle panel is the corresponding [N 2] 6584 $P-V$ and [O 3] on the left panel. Spatial offsets are in arcseconds. We show the image plus slits on the left bottom panel. The stellar continuum from the central star has not been subtracted. We derive a heliocentric systemic velocity, $V_{\text{sys}} = 70.5 \text{ km s}^{-1}$ by using the slits position f (epoch 2003) and which passes near through the central star.

References

- L  pez, J. A., Richer, M. G., Garc  a-D  az, M. T., Clark, D. M., Meaburn, J., Riesgo, H., Steffen, W., & Lloyd, M. 2012, RevMexAA, 48, 3
- Meaburn, J., L  pez, J. A., Guti  rrez, L., Quir  z, F., Murillo, J. M. & Vald  z, J. 2003, RMxAA, 39, 185M
- Balick B., Alexander J., Hajian A. R., Terzian Y., Perinotto M., & Patriarchi P. 1998, ApJ, 116, 360
- Balick, B., Preston, H. L., Icke, V. 1987a, AJ, 94, 1641B
- Balick B., Owen R., Bignell C. R., Hjellming R. M. 1987b, AJ, 94, 948
- Balick B. 1987c, AJ, 94, 671
- Ciardullo, R., Bond, H. E., Sipior, M. S., Fullton, L. K., Zhang, C.-Y., Schaefer, K. G. 1999, AJ, 118, 488
- Clark, D. M., Garc  a-D  az, M. T., L  pez, J. A., Steffen, W. G., & Richer, M. G. 2010, ApJ, 722, 1260
- Danehkar, A., Frew, D. J.; De Marco, O., & Parker, Q. A. 2011, arXiv1109.2181D
- Frew, D. J. 2008, Ph.D. Thesis, Department of Physics, Macquarie University, NSW, 2109, Australia
- Garc  a-D  az, M. T., Clark, D. M., L  pez, J. A., Steffen, W., & Richer, M. G. 2009, ApJ, 699, 1633
- Garc  a-D  az, Ma. T., & Henney, W. J. 2007, AJ, 133, 952G
- Giesecking, F., Becker, I., & Solf, J. 1985, ApJ, 295L, 17G
- Guerrero, M. A., Chu, Y.-H., Gruendl, R. A., & Meixner, M. 2005, A&A, 430L, 69
- Heap, S. R. 1977, ApJ, 215, 864
- Kastner et al. 2012, arXiv:1204.6055
- Kudritzki, R. P., Mendez, R. H., Puls, J., McCarthy, J. K. 1997, IAUS, 180, 64
- L  pez, J. A., Garc  a-D  az, M. T., Steffen, W., Riesgo, H. & Richer, M. G. 2012a, ApJ, 750, 131
- M  ndez, R. H., Urbaneja, M.A., Kudritzki, R. P. & Prinja, R. K. 2011, IAUS 283, submitted.
- Natta, A., Pottasch, S. R., & Preite-Martinez, A., 1980, A&A, 84, 284
- O'Dell, C. R., Balick, B., Hajian, A. R., Henney, W. J. & Burkert, A. 2002, AJ123, 3329
- O'Dell, C. R., Weiner, L. D., & Chu, Y. H. 1990, ApJ, 362, 226
- O'Dell, C. R., & Ball, M. E. 1985, ApJ, 289, 526
- Pauldrach, A. W. A., Hoffmann, T. L., & Mendez, R. H. 2004, A&A, 419, 1111
- Phillips, J. P., & Cuesta, L. 1999, AJ, 118, 2929
- Pottasch, S. R., Bernard-Salas, J., & Roelling T. L. 2008, A&A, 481, 393
- Reed, D. S., Balick, B., Hajian, A. R., Clayton, T. L., Giovanardi, S., Casertano, S., Panagia, N., & Terzian, Y. 1999, AJ, 118, 2430
- Stanghellini, L. & Shaw, R. A. 2008, ApJ, 689, 194
- Steffen, W., Koning, N., Wenger, S., Morisset, C., & Magnor, M. 2010, IEEE, Transactions on Visualization and Computer Graphics, 17, No. 4, 454
- Steffen, W., Esp  ndola, M., Mart  nez, S., & Koning, N. 2009, RMxAA, 45, 143
- Steffen, W. & L  pez, J. A. 2006, RMxAA, 42, 99
- Tinkler, C. M., Lamers, H. J. G. L. M. 2002, A&A, 384, 987
- Weedman, D. W. 1968, ApJ, 153, 49
- Zhang, Y., Fang, X., Chau, W., Hsia, C.-H., Liu, X.-W., Kwon, S., & Koning, N. 2012, arXiv:1205.3470

¹ IRAF is distributed by the National Optical Astronomy Observatory, which is operated by the Association of Universities for Research in Astronomy, Inc. under cooperative agreement with the National Science foundation

Table 1. Log of Time-resolved Observations of NGC 6210.

Run DD/MM/YYYY	Spectroscopy hight resolution/ 2.1m OAN-SPM						
	No. of frame	Exp. Time (s)	Range (Å)	Resolution (Å)	slit (mμ)	P. A. (degree)	slit name
28/06/1998	1	30	Hα	0.26	90	150	o
28/06/1998	1	300	Hα	0.26	90	150	n
28/06/1998	3	1200	Hα	0.26	90	150	m,p,q
05/06/2003	7	1800	Hα	0.26	70	0	f,e,d,h,i,k,b
16/10/2003	1	1800	Hα	0.26	70	21	t
16/10/2003	1	1800	Hα	0.26	70	68	v
17/10/2003	1	1800	Hα	0.26	70	77	w
13/06/2004	1	1800	OIII	0.19	70	9	r
13/06/2004	1	1800	OIII	0.19	70	19	s
14/06/2004	1	1800	SII	–	150	19	s
13/06/2004	1	1800	OIII	0.19	70	56	u
14/06/2004	2	1800	OIII	0.19	150	0	a,l
21/05/2011	1	1800	Hα	0.26	150	0	g
21/05/2011	1	6000	OIII	0.19	150	0	g
06/07/2013	3	1800	Hα	0.26	150	0	c,i,j

Table 2. Log of Time-resolved Observations of NGC 6210. Epoch 2015

Run DD/MM/YYYY	Spectroscopy hight resolution/ 2.1m OAN-SPM						
	No. of frame	Exp. Time (s)	Range (Å)	Resolution (Å)	slit (mμ)	P. A. (degree)	slit name
18/08/2015	5	1800	Hα, [OIII]	0.26	70	0	c, d, e, f, g
19/08/2015	3	1800	Hα, [OIII]	0.26	70	0	b, a, i
20/08/2005	3	1800	Hα, [OIII]	0.26	70	0	h, j, k

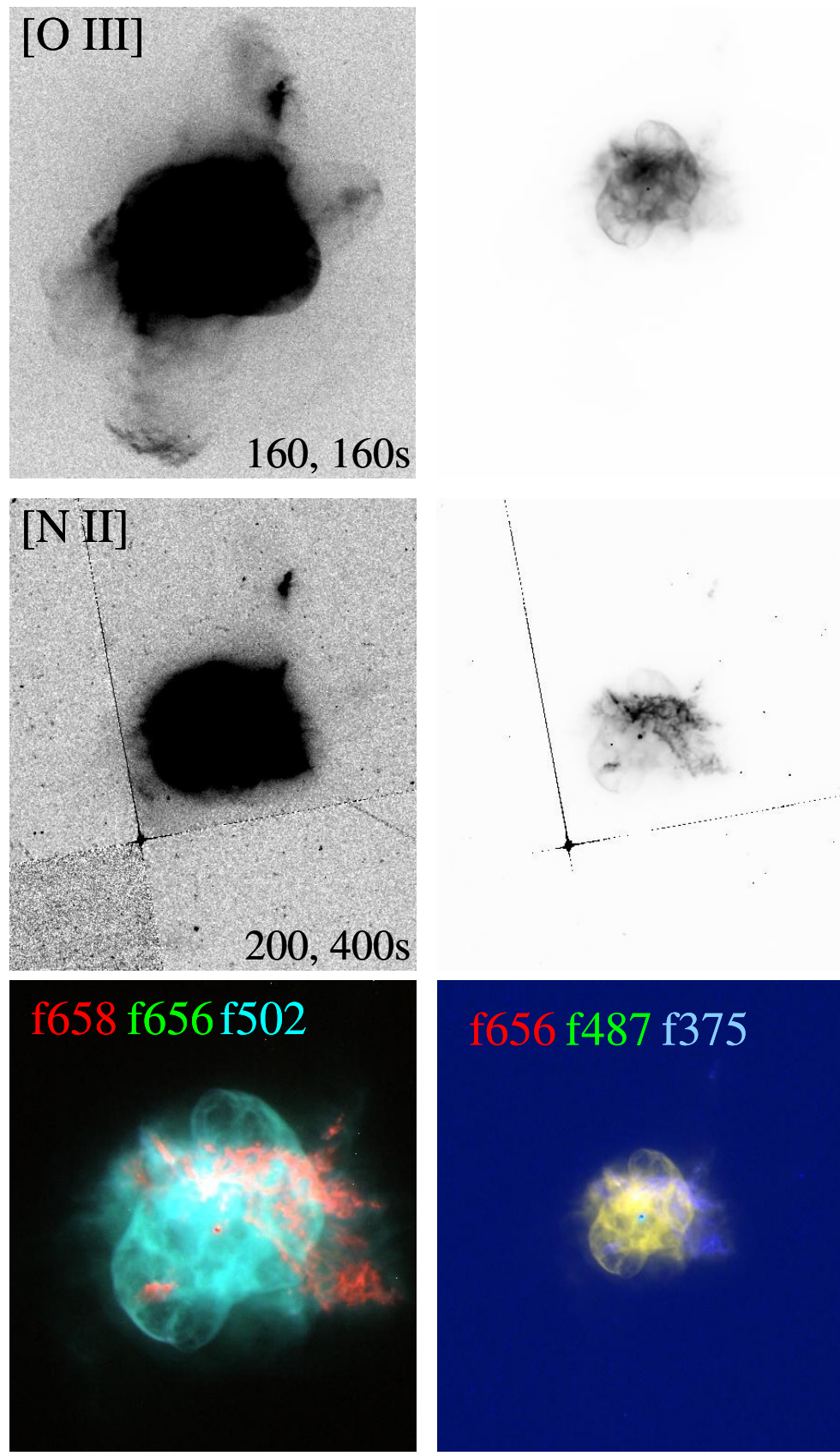


Fig. 1.

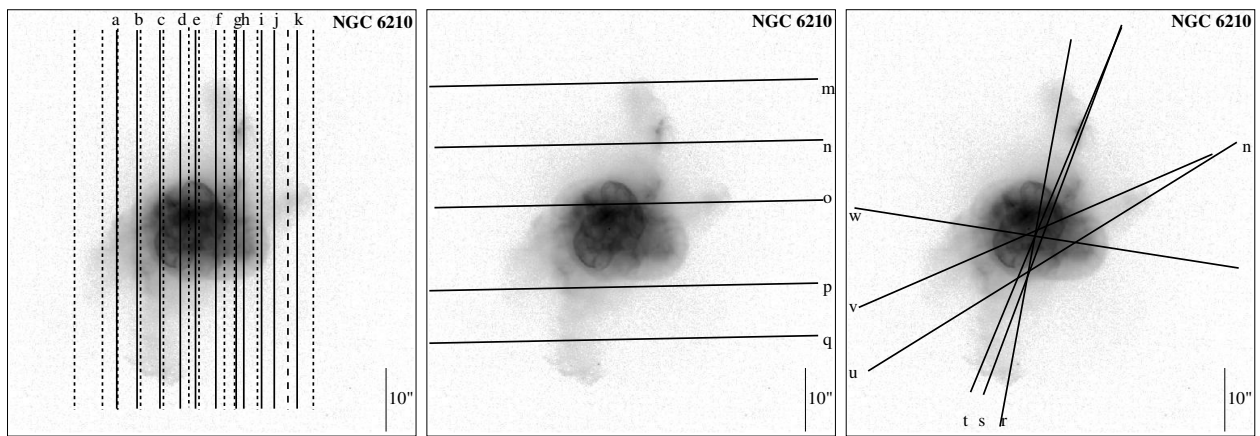
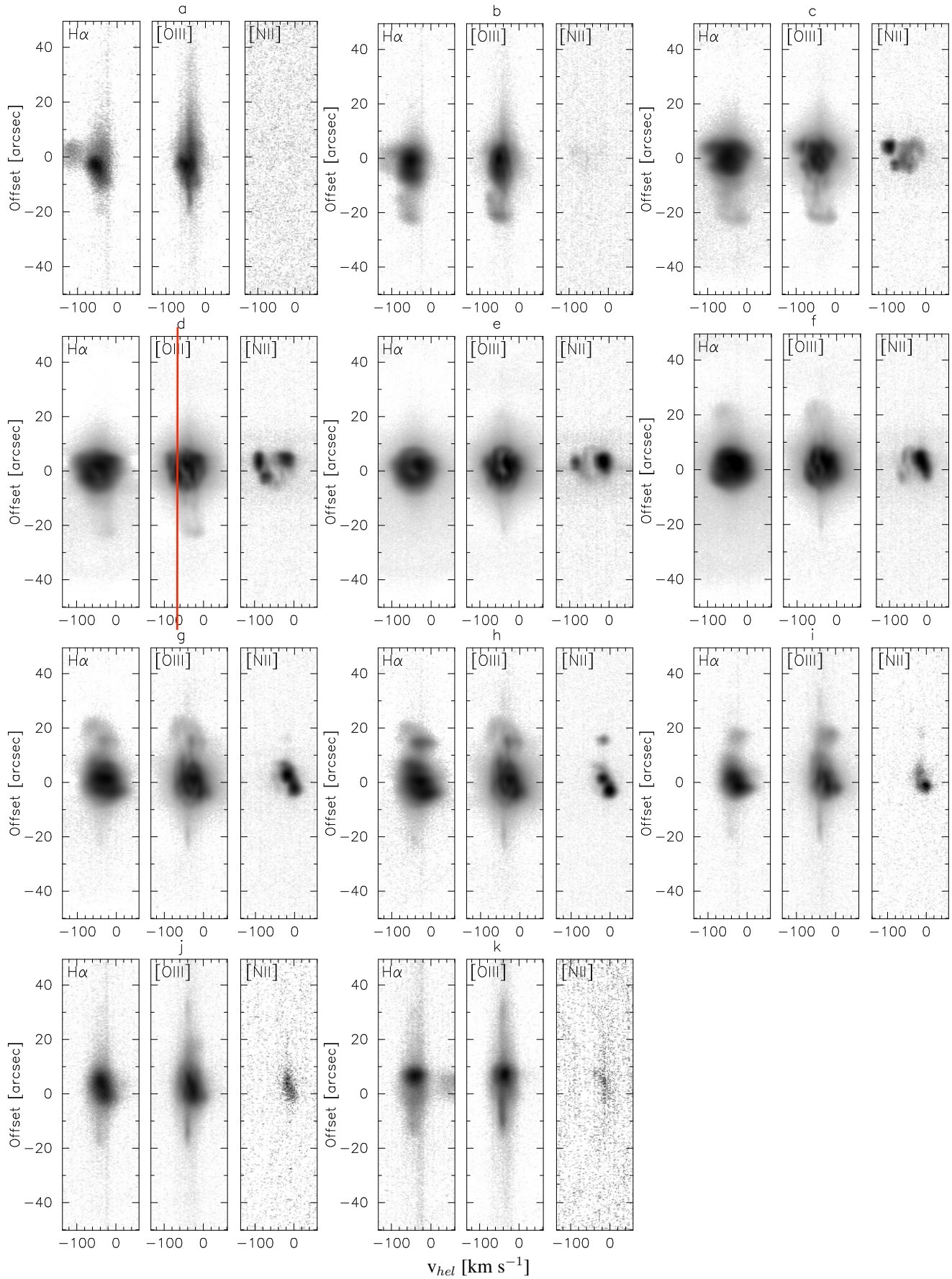


Fig. 2.

**Fig. 3.**

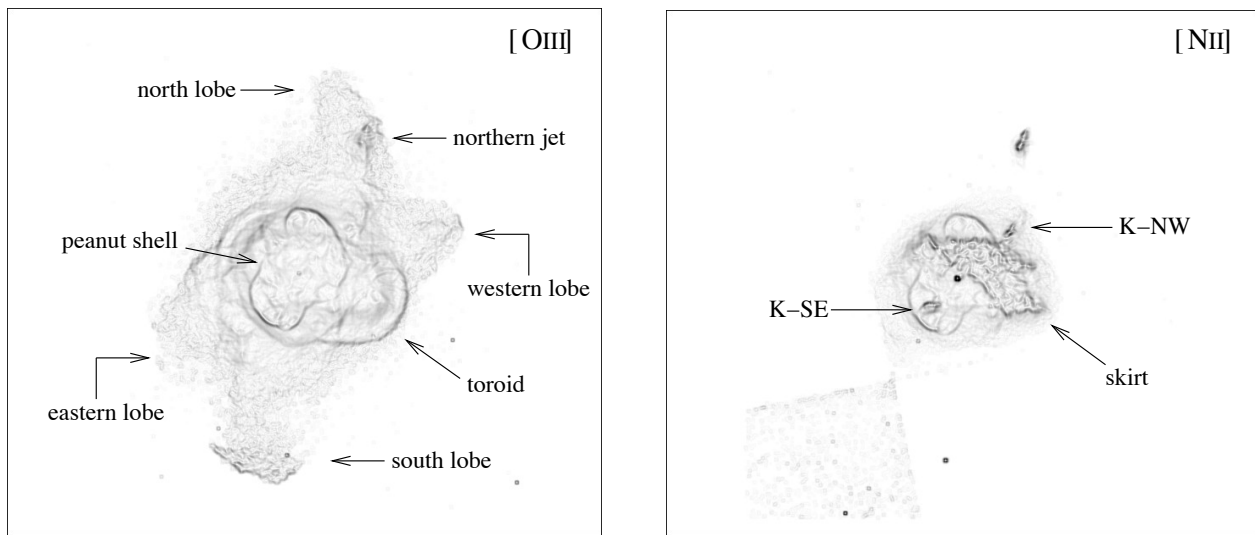


Fig. 4.

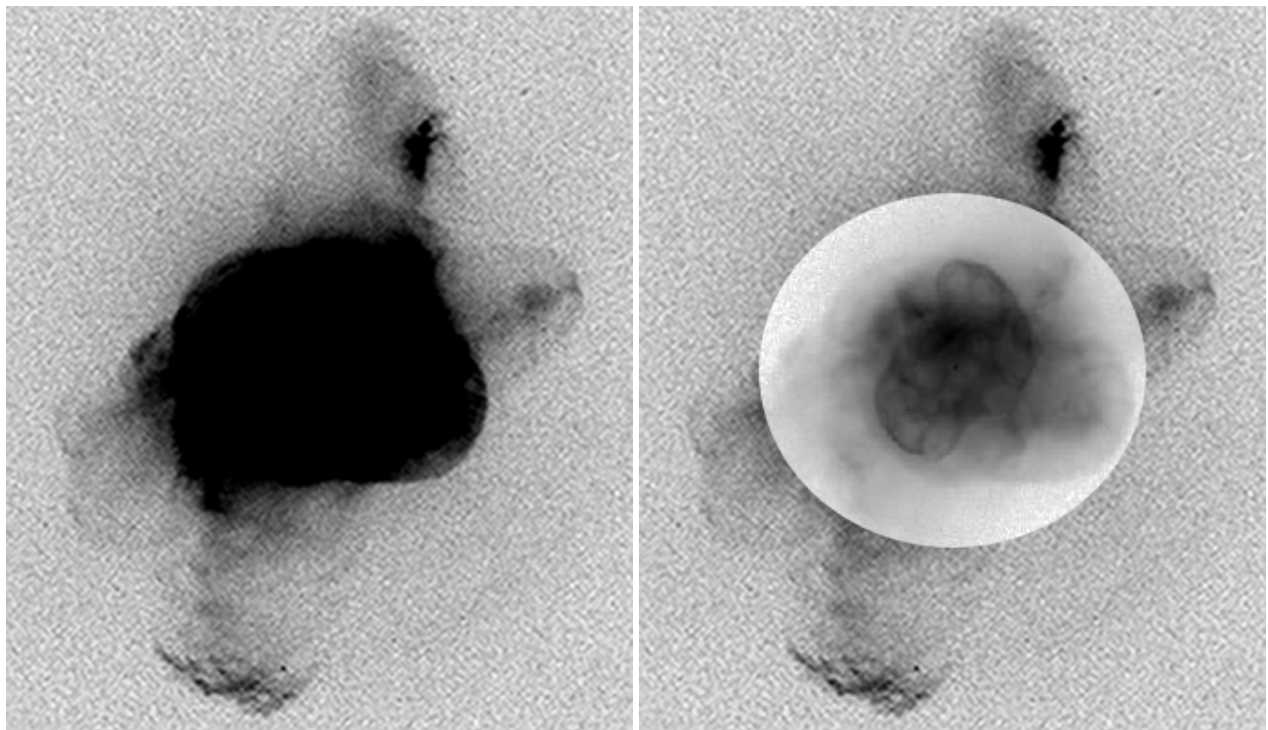
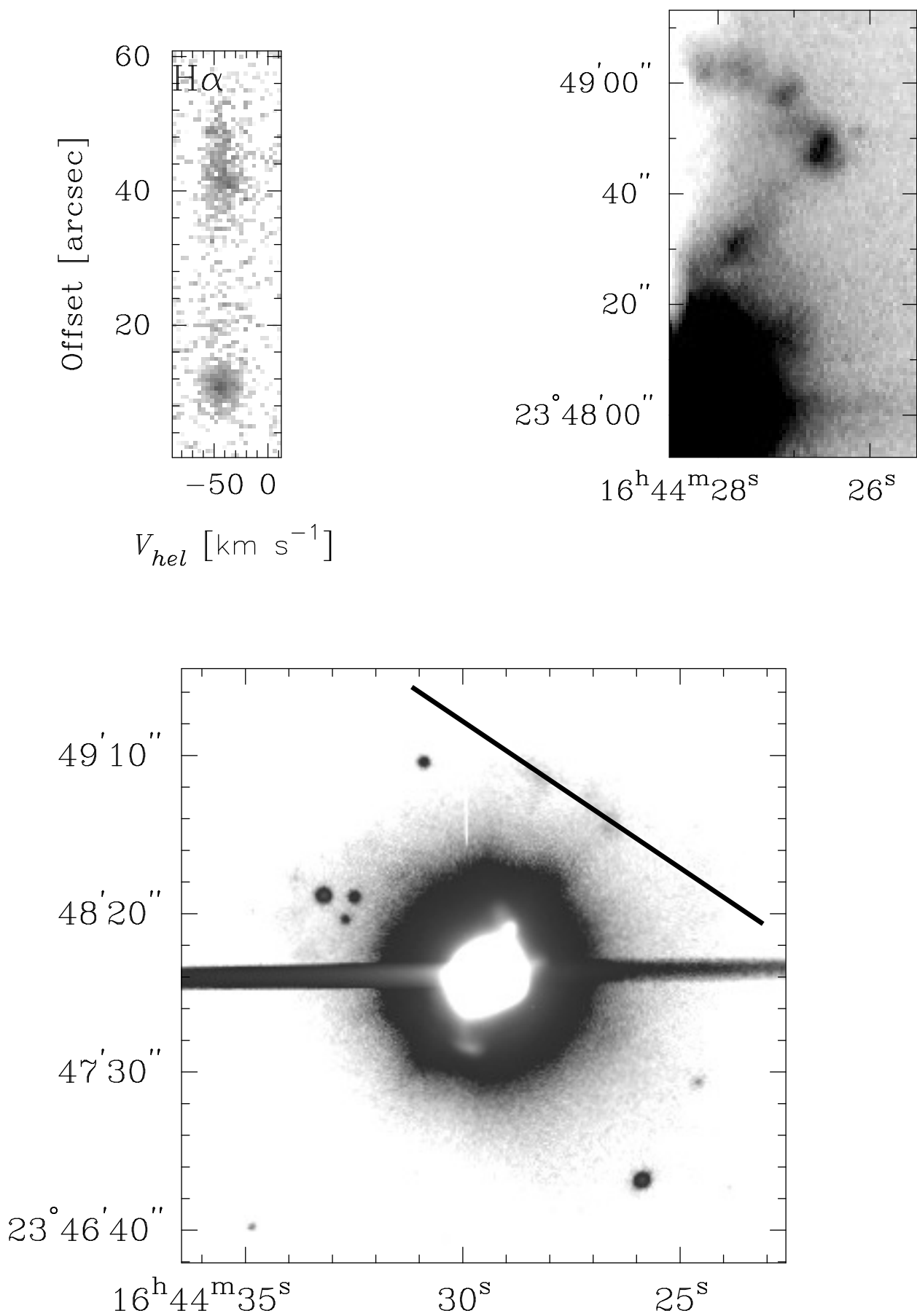


Fig. 5.

**Fig. 6.**

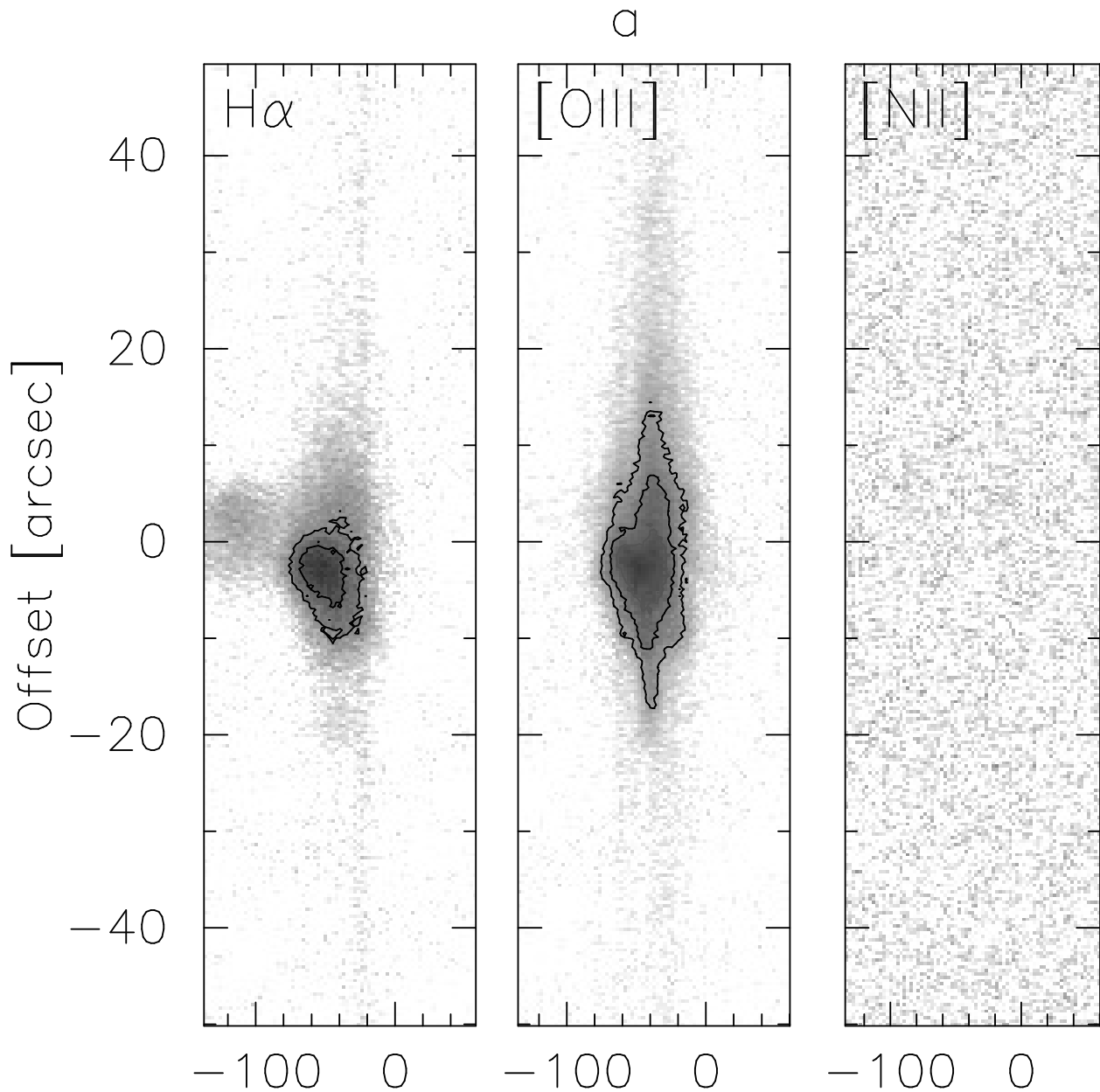


Fig. 7.

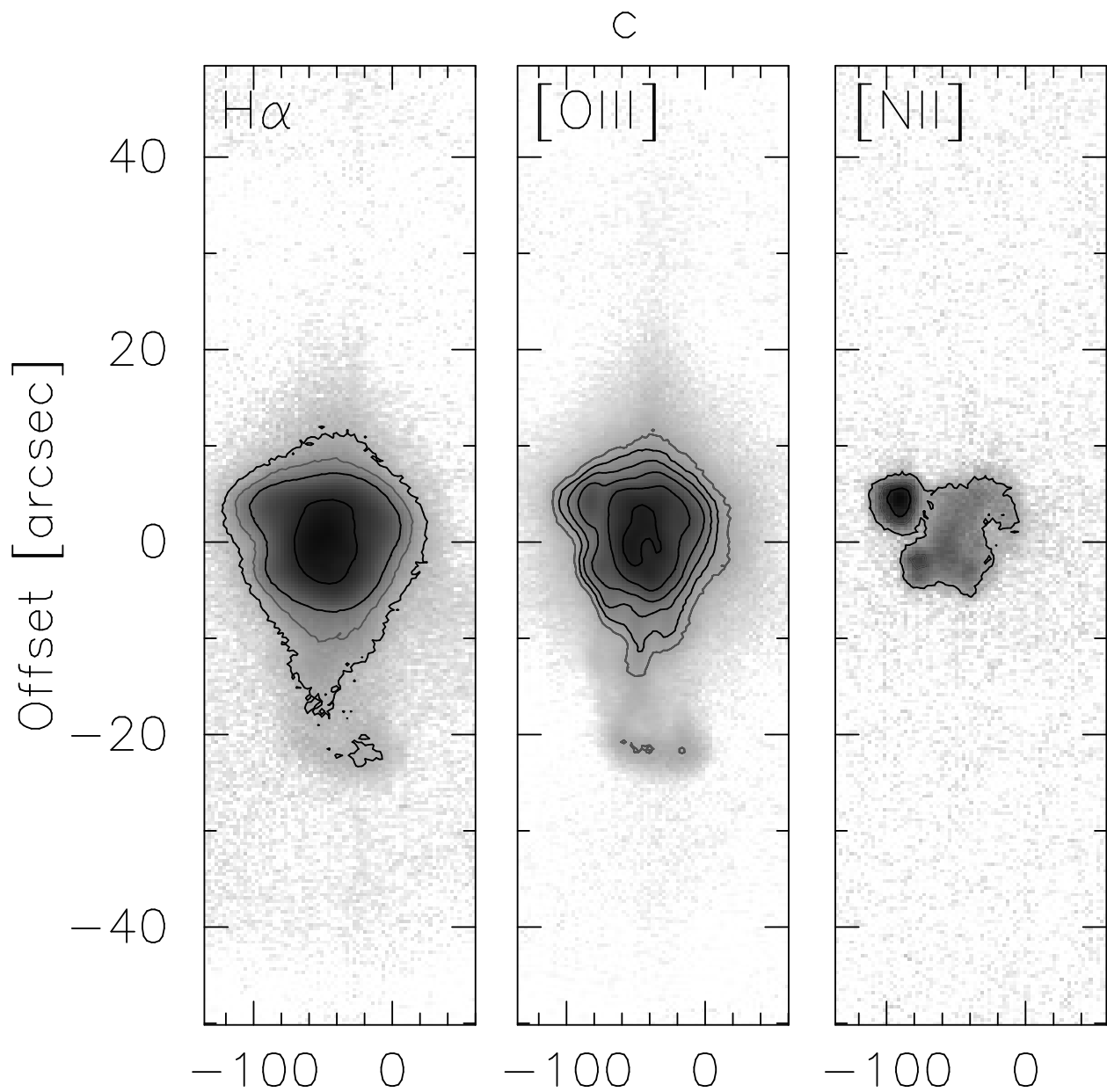


Fig. 8.

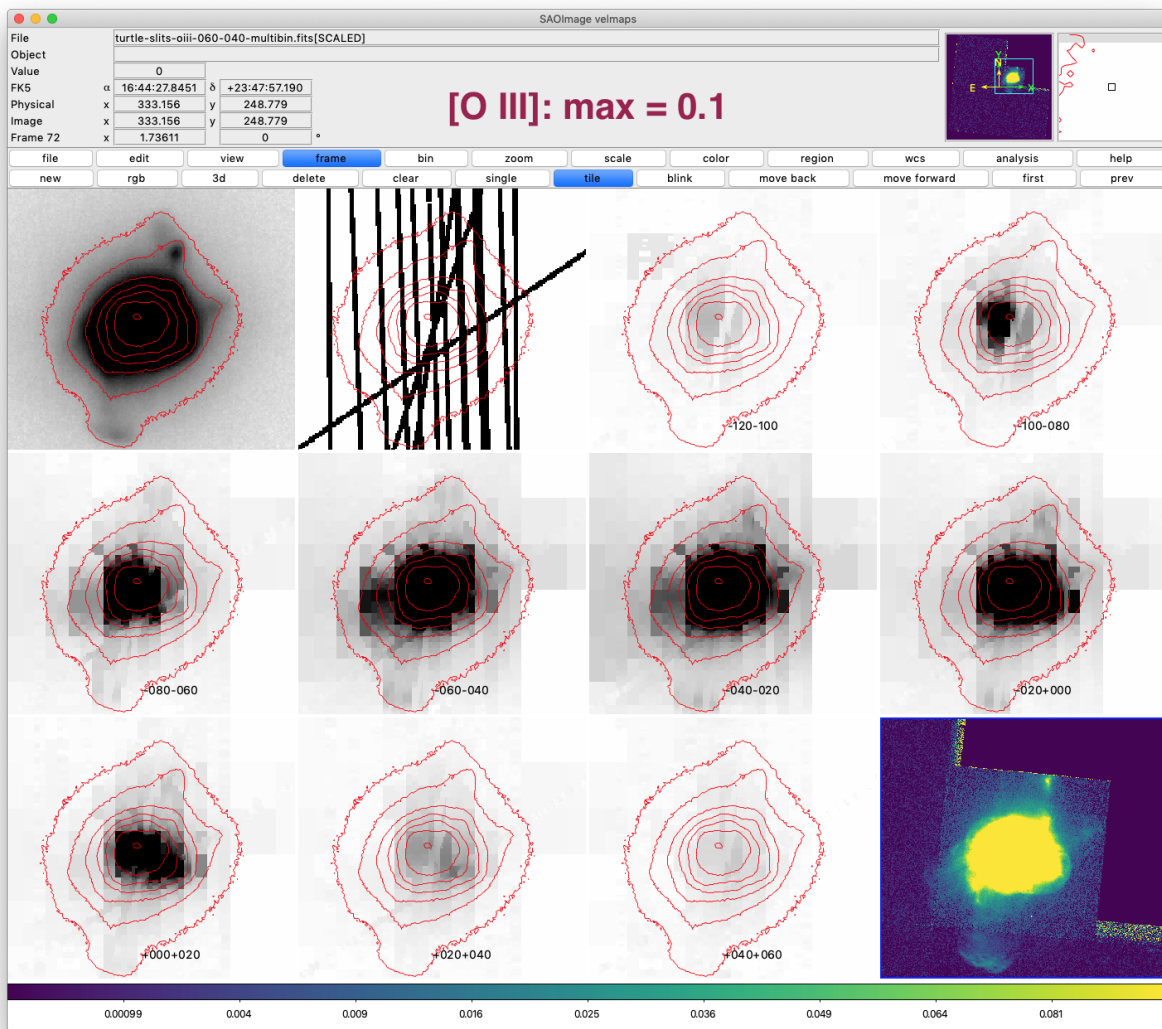
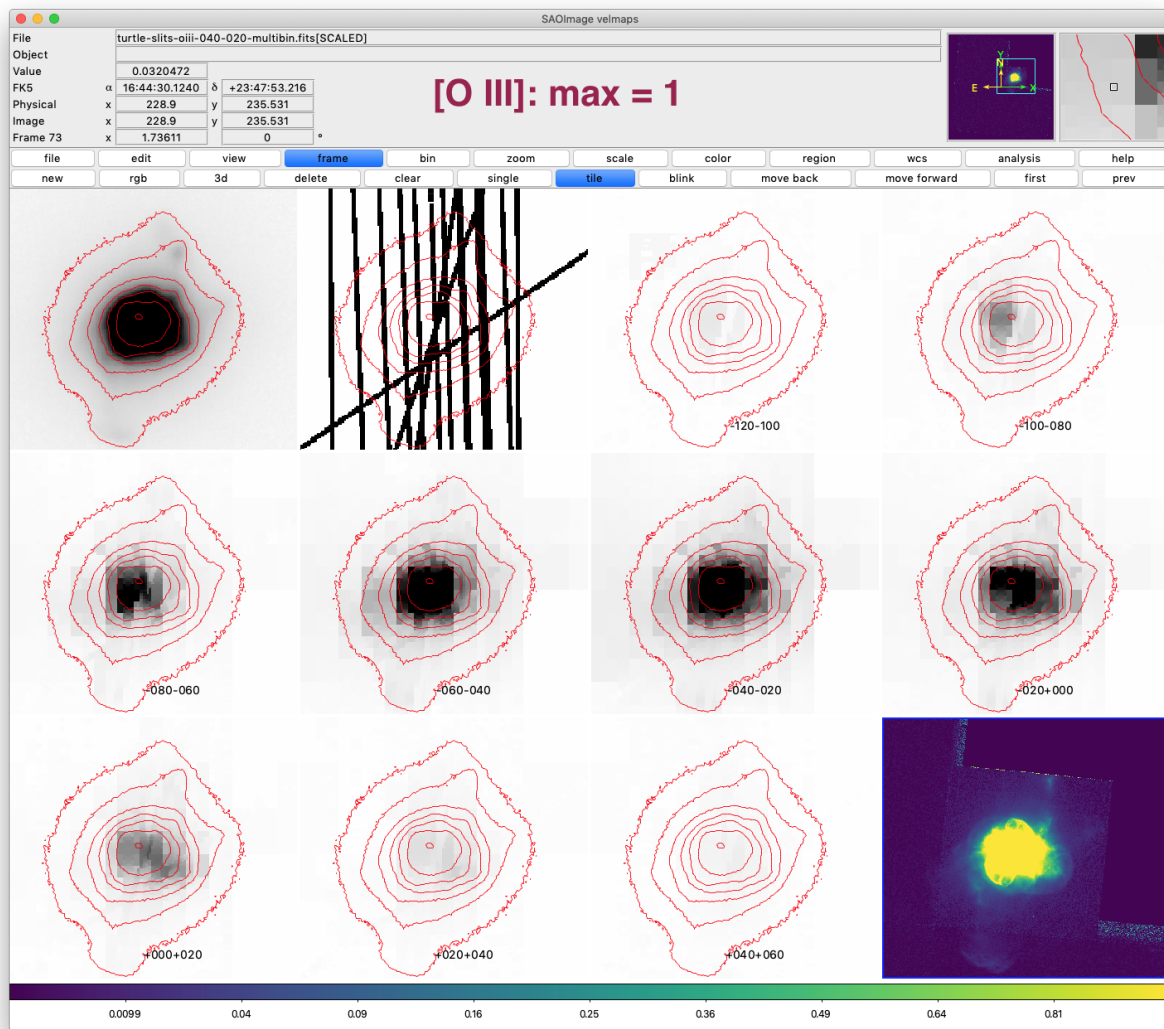


Fig. 9. los canales son de 20 km/s, con límites heliocéntricos marcados. El panel 1 es la imagen mediana de [O III] construida de todas las exposiciones I+S. El panel 2 muestra las posiciones de las rendijas, que te da una idea de la resolución efectiva en RA. Y el último, en color, es la imagen HST en [O III]

**Fig. 10.**

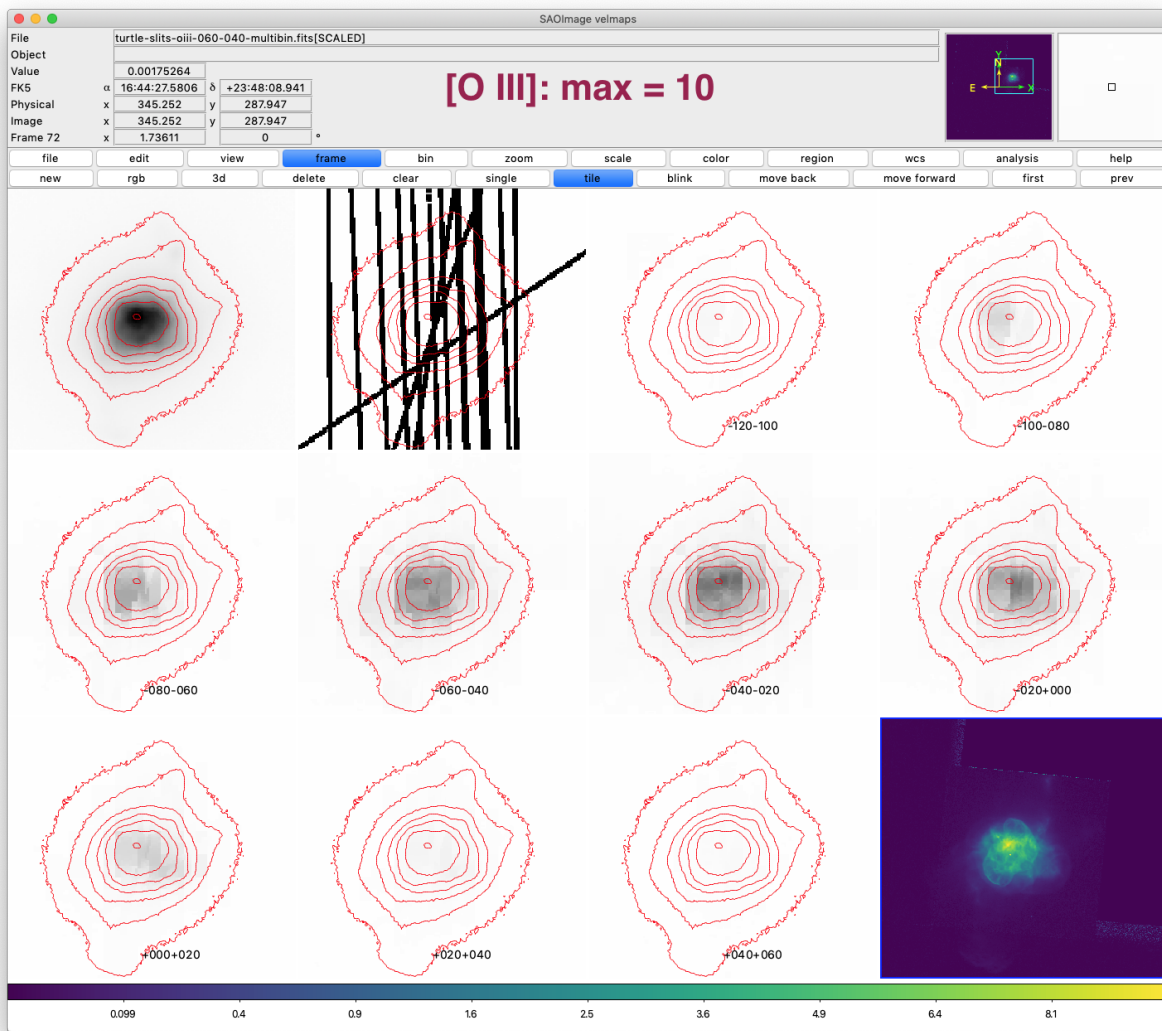
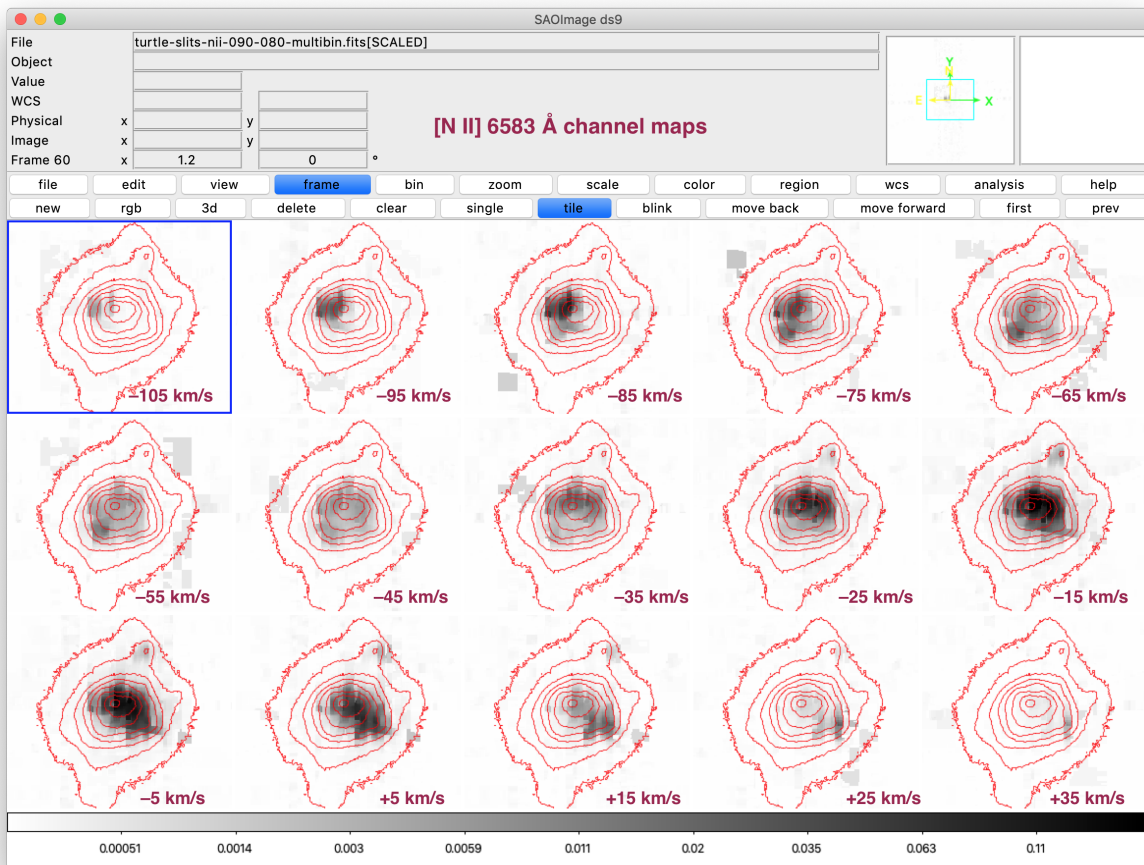


Fig. 11.

**Fig. 12.**

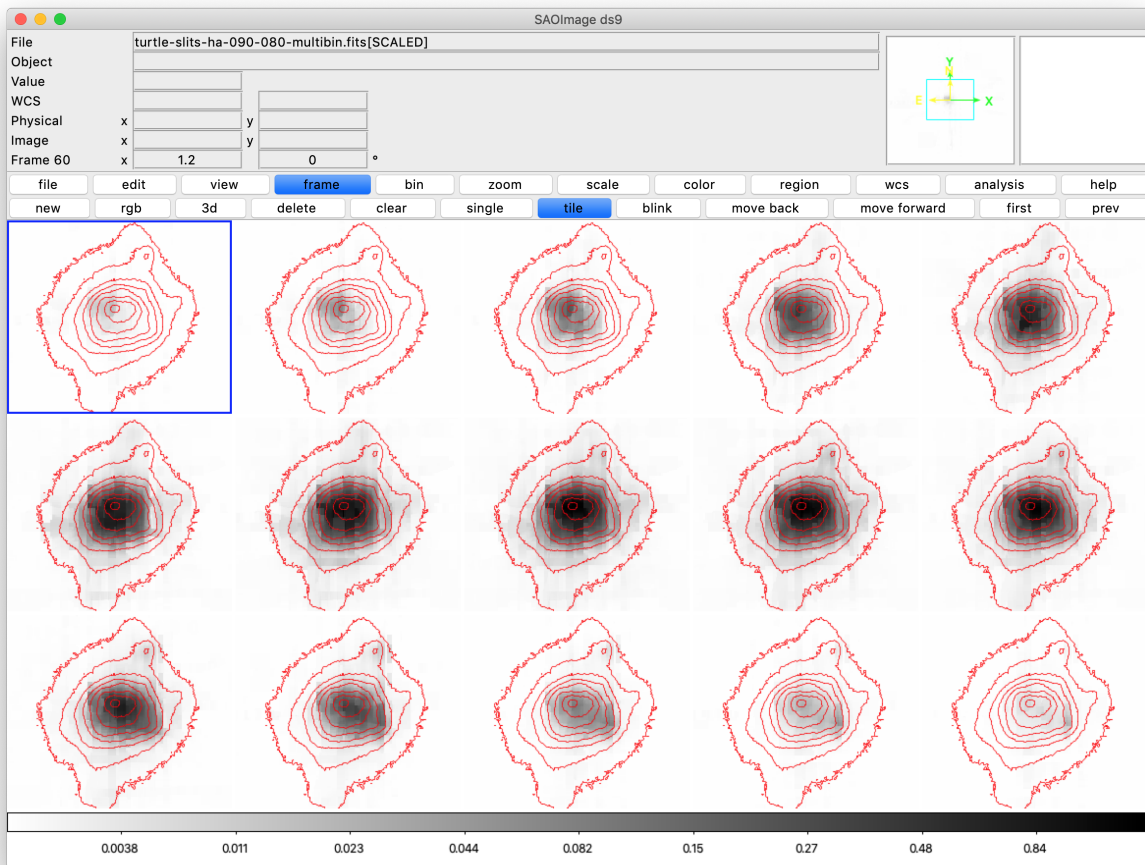


Fig. 13.